Dynamics and command shaping control of quadcopters carrying suspended loads

Sarah Ichikawa * **Arnoldo Castro** ** **Nicholas Johnson** **
Hirohisa Kojima * **William Singhose** **

* *Tokyo Metropolitan University, Department of Aerospace Engineering, Tokyo, Japan*
** *Georgia Institute of Technology, School of Mechanical Engineering, Atlanta, GA (Singhose@gatech.edu)*

Abstract: Quadrotors have proven to be a versatile class of machines with many applications. Quadrotors carrying suspended loads exhibit an oscillatory mode much like a crane. However, the swinging payload can greatly disturb the quadrotor and lead to control difficulties and instability. A dynamic model of a quadrotor carrying a suspended payload is presented. The dynamic model is used to demonstrate the effect of system parameters and move distances on the dynamic response. Various types of input-shaping control are also investigated as a method to reduce swing and improve control performance.

Keywords: Quadrotor, Command Shaping, Suspended Payload

1. INTRODUCTION

One challenging application for a quadrotor is to transport a cable-suspended payload. When carrying such a suspended payload, the quadrotor motion induces payload swing. The resulting payload oscillation can damage the payload or its environment by colliding with obstacles. Additionally, the swinging payload creates disturbance forces that can significantly effect the motion of the main quadrotor body. Hence, it is necessary to utilize a control method that is stable and can limit payload oscillations.

In this paper, an input-shaping approach that generates commands for canceling residual oscillation is evaluated [Singer and Seering (1990), Tallman and Smith (1958), Smith (1958)]. Klausen et al. (2017) developed a nonlinear hexacopter tracking controller that compensates for wind disturbance, and generated swing-free trajectories using input shaping. Homolka et al. (2017) applied input command shapers on a 2-dimentional quadrotor model. Sadr et al. (2014) developed a model based algorithm (MBA) controller combined with an anti-swing controller based on input shaping. They examined the use of the Zero Vibration (ZV) shaper and the Zero Vibration and Derivative (ZVD) shaper.

2. QUADROTOR DYNAMIC MODEL

2.1 Coordinate definition and transformation

A schematic diagram of a quadrotor with a suspended payload and definition of angles is shown in Fig. 1. The position of the quadrotor in the inertial frame is $\mathbf{r} = [\mathbf{x}\ \mathbf{y}\ \mathbf{z}]^{\mathbf{T}}$ and attitude of the quadrotor is represented in the form of Euler angles $\xi = [\phi\ \theta\ \psi]^{\mathbf{T}}$.

The Z-X-Y rotational matrix from the body frame of the quadrotor to the inertial frame, R, is:

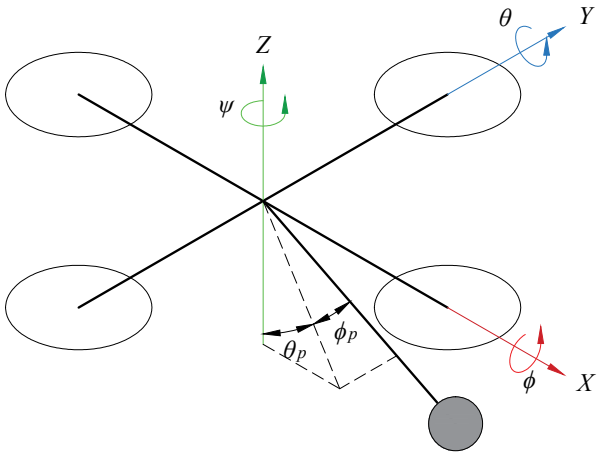

Fig. 1. A schematic diagram of a quadrotor with a suspended payload.

$$R = \begin{bmatrix} c_\theta c_\psi - s_\phi s_\theta s_\psi & -c_\phi s_\psi & c_\psi s_\theta + c_\theta s_\phi s_\psi \\ c_\theta s_\psi + c_\psi s_\phi s_\theta & c_\phi c_\psi & s_\psi s_\theta - c_\psi c_\theta s_\phi \\ -c_\phi s_\theta & s_\phi & c_\phi c_\theta \end{bmatrix} \quad (1)$$

where $c_x = \cos x$ and $s_x = \sin x$.

2.2 Control Inputs

The control input consists of the total thrust of quadrotor T and torque τ. Those are expressed as [Derafa et al. (2006)]:

$$T = k_1\omega_1^2 + k_2\omega_2^2 + k_3\omega_3^2 + k_4\omega_4^2 \quad (2)$$

$$\tau = \begin{bmatrix} \tau_\phi \\ \tau_\theta \\ \tau_\psi \end{bmatrix} = \begin{bmatrix} lk_1\omega_3^2 - lk_3\omega_1^2 \\ lk_2\omega_4^2 - lk_4\omega_2^2 \\ b_1\omega_1^2 - b_2\omega_2^2 + b_3\omega_3^2 - b_4\omega_4^2 \end{bmatrix} \tag{3}$$

where k_i, ω_i and b_i are the thrust coefficient, angular velocity, and torque coefficient of each motor, respectively, and l is the length from the center of mass of the quadrotor to the center of the motor.

2.3 Suspended Payload Dynamics

We assume that the quadrotor flies in low-wind conditions, thus we neglect the effect of such disturbances. We adopt the model used in Johnson (2017). The translational and rotational dynamic equations of the quadrotor are expressed as:

$$\ddot{r} = \frac{1}{m_q}\left(F_g + F_d + RT_r + RF_p\right) \tag{4}$$

$$\ddot{\xi} = \mathbf{I}^{-1}\left(\tau_d + \tau + \tau_p - \dot{\xi} \times (\mathbf{I}\dot{\xi})\right) \tag{5}$$

where m_q is mass of the quadrotor, F_g is the gravitational force, F_d is the drag force vector, T_r is the thrust vector, F_p is the payload tension, I is the moment of inertia of the quadrotor, τ_d is the torque caused by drag, and τ_p is the torque caused by the payload tension. F_g,F_d,T_r,τ_d, and τ_p are given by:

$$\begin{aligned} F_g &= [0\ 0\ -m_q\ g]^T \\ F_d &= -\frac{1}{2}C_d A \rho_{air} |\dot{r}| \dot{r} \\ T_r &= [0\ 0\ T]^T \\ \tau_d &= (Rr_{cop}) \times F_d \\ \tau_p &= R(r_{susp} \times F_p) \end{aligned} \tag{6}$$

where g is gravity acceleration in the inertial frame, C_d is the drag coefficient, A is the area that is exposed for drag consideration, ρ_{air} is air density, r_{cop} is the relative vector from the center of pressure and the center of gravity of the quadrotor in the body frame, and r_{susp} is the length of suspension offset in the body frame. Lastly, F_p can be expressed as follows under small angle approximations:

$$F_p = -m_p g_\xi \tag{7}$$

where m_p is the payload mass and g_ξ is the acceleration of gravity in the body frame.

3. CONTROL SYSTEM

A quadrotor with a suspended payload creates control challenges far exceeding those of an unloaded quadrotor because of load-attitude coupling. This means that the suspended load creates a disturbance force on the main body of the quadrotor. However, it also adds an additional oscillatory mode.

3.1 Input shaping

Input shaping is a technique that can reduce oscillations when the period of oscillations is only approximately known. The period of the suspended payload swing, T_d can be approximated as $T_d = 2\sqrt{(L_p/g)}$ where L_p is the cable length that suspends a payload. Note that this estimation applies when the payload is fairly light compared to the main body of the quadrotor.

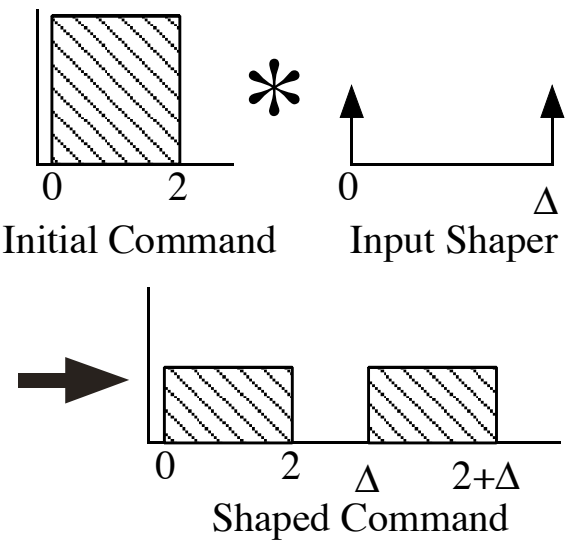

Fig. 2. Command generation process.

To explain the general idea of input shaping, the ZV shaper, which consists of two impulses, is explained here. The first impulse will cause the system to oscillate and then applying the second impulse at the correct time will cancel the oscillation [Smith (1958)]. The second impulse has to be given to the system at the appropriate time, which is half of the period of an oscillation. Input-shaped commands are generated by convolving the input shaper with the baseline input command.

This command generation process is demonstrated in Figure 2 using a 2-second pulse as the initial command. Note that the convolution product in this case is a two-pulse command. For the case shown in Figure 2, the shaper duration, Δ, is longer than the initial command, but in most cases the impulse sequence will be much shorter than the baseline command profile. This is especially true when the system is moving through a complex trajectory and the period of system vibration is small compared to the duration of the move. When this is the case, the shaped command will form a continuous function, as shown in Figure 3.

Zero-vibration (ZV) shaped commands Smith (1958), negative zero-vibration (NZV) commands [Singhose et al. (1997a)], extra insensitive (EI) commands [Singhose et al. (1994)], and 2-hump EI shaped commands [Singhose et al. (1997b)] were evaluated for the oscillation control of the payload in this study.

Let the amplitude of impulse be A_i and its timing be t_i, where i is the index. Then, the ZV shaper is given by:

$$\text{ZV shaper} \begin{bmatrix} A_i \\ t_i \end{bmatrix} = \begin{bmatrix} 0.5 & 0.5 \\ 0 & \frac{T_d}{2} \end{bmatrix} \tag{8}$$

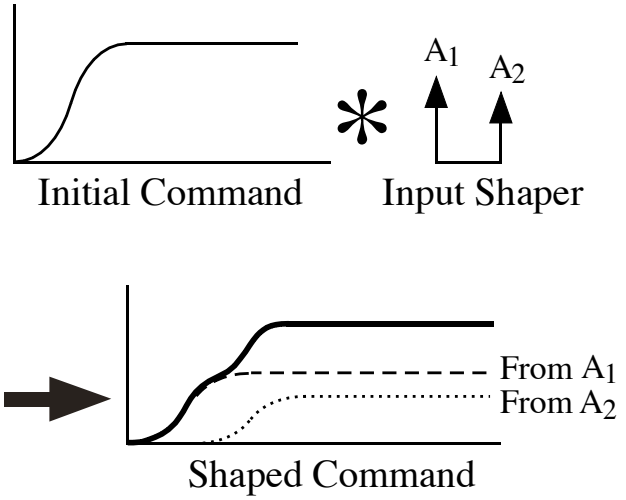

Fig. 3. Shaped lcommand.

The NZV shaper has two positive impulses and a negative impulse between them. Its characteristic is that its duration is only one third of the period, which is 33 % faster than the positive ZV shaper in (8).

$$\text{NZV shaper} \begin{bmatrix} A_i \\ t_i \end{bmatrix} = \begin{bmatrix} 1 & -1 & 1 \\ 0 & \frac{T_d}{6} & \frac{T_d}{3} \end{bmatrix} \tag{9}$$

Although the EI shaper has a duration of only one period of oscillation, it is a very robust shaper achieved by utilizing a tolerable value limit, V_{tol}. Its impulses are:

$$\text{EI shaper} \begin{bmatrix} A_i \\ t_i \end{bmatrix} = \begin{bmatrix} \frac{1+V_{tol}}{4} & \frac{1-V_{tol}}{2} & \frac{1+V_{tol}}{4} \\ 0 & \frac{T_d}{2} & T_d \end{bmatrix} \tag{10}$$

The 2-hump EI shaper is an extended version of the EI shaper and it is given by:

$$\text{2-hump EI shaper} \begin{bmatrix} A_i \\ t_i \end{bmatrix} = \begin{bmatrix} A_1 & \frac{1}{2}-A_1 & \frac{1}{2}-A_1 & A_1 \\ 0 & \frac{T_d}{2} & T_d & \frac{3}{2}T_d \end{bmatrix} \tag{11}$$

where,

$$A_1 = (3X^2 + 2X + 3V_{tol}^2)16X, \quad X = \sqrt[3]{V_{tol}^2\sqrt{1-V_{tol}^2}+1} \tag{12}$$

The robustness qualities of shapers can be displayed by showing their robustness curves. Such curves display the amount of residual vibration versus the system frequency, or error in the system frequency. When the system frequency is known well, the residual vibration will be small. When the error in frequency increases, the residual vibration will, in general, increase. The robust shapers allow a much larger error in frequency before the residual vibration becomes large. The sensitivity curves for the ZV, ZVD, and EI shapers are shown in Figure 4. The sensitivity curves for the 2-Hump EI and ZVDD shaper Singer and Seering (1990) are shown in Figure 5.

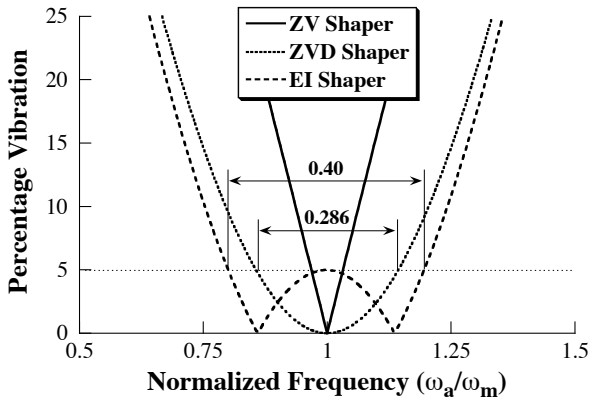

Fig. 4. Sensitivity curves for the ZV, ZVD, and EI shapers.

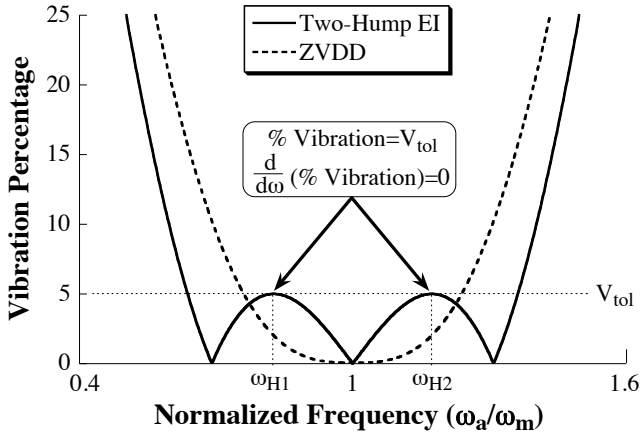

Fig. 5. Sensitivity curves for the 2-Hump EI and ZVDD shapers.

Although, robust shapers greatly increase the amount of tolerable modeling error, they tend to increase the system rise time. The rise time increase is proportional to the duration of the input shaper. When given the task of designing an input shaper, a controls engineer will be faced with a trade-off between robustness and rise time. Figure 6 provides information about the time cost of obtaining a desired level of 5% insensitivity, where insensitivity, I, is the nondimensional width of the sensitivity curve that is below the tolerable vibration limit - 5% vibration in this case.

Figure 7 shows the ratio of (5% insensitivity)/(shaper duration) as a function of the insensitivity. The local maximum points labeled by ZV, EI, and two-hump EI shapers indicate that if the desired insensitivity range includes one of these points, then those shapers are good choices.

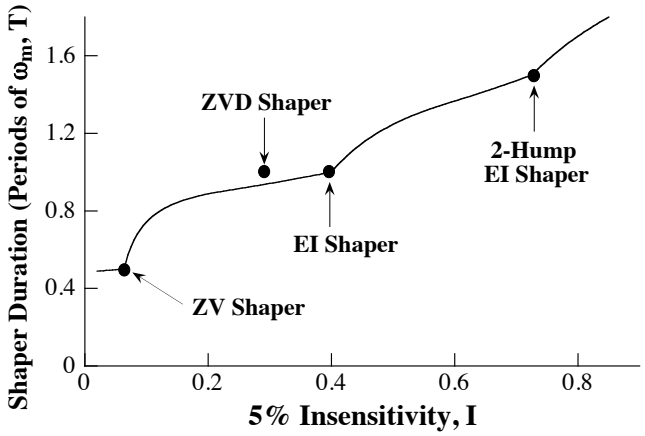

Fig. 6. Tradeoff between duration and shaper robustness.

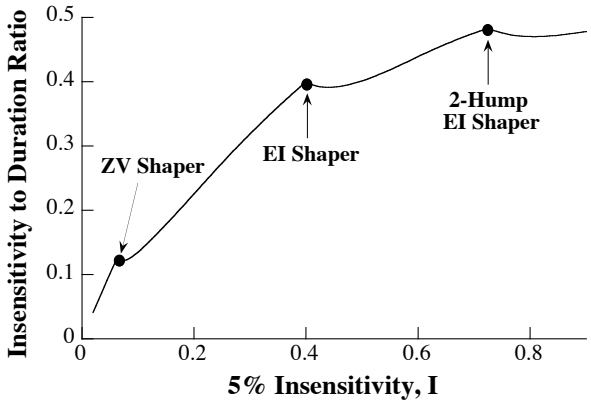

Fig. 7. Ratio of (5% insensitivity)/(shaper duration) as a function of the insensitivity.

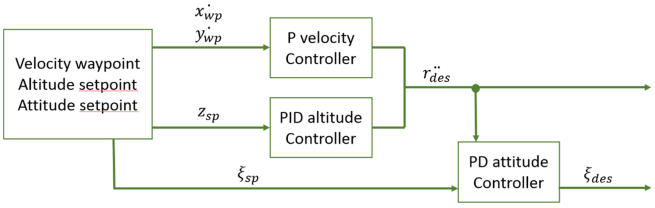

Fig. 8. Quadrotor controller scheme

3.2 Quadrotor controller

Our quadrotor simulation includes a PD attitude controller, P velocity controller in the x and y directions, and PID altitude controller. The overall feedback controller structure is shown in Fig. 2. Subscripts wp, sp, and des denote waypoint, setpoint, and desired, respectively. The controller gains were tuned manually.

Input shaping can be implemented with velocity control or attitude control. Considering that usual transportation cases require a quadrotor to move a specific distance or move with a specific velocity, this paper focuses on applying input shaping to velocity control.

The gains of the attitude controller are $K_{Px} = K_{Py} = K_{Pz} = 0.9$ and $K_{Px} = K_{Py} = K_{Pz} = 0.28$. The gains of the velocity controller are $K_{Px} = K_{Py} = 1.2$ and $K_{Pz} = 0$. The altitude controller gains are $K_{Px} = K_{Py} = 12$, $K_{Ix} = K_{Iy} = K_{Iz} = 1$ and $K_{Dx} = K_{Dy} = K_{Dz} = 6$. Physical parameters used for the simulations are shown in Table 1.

Table 1. Simulation parameters

Parameters	Values
m_q (kg)	1
I_{xx} (kg·m^2)	6.816×10^{-3}
I_{yy} (kg·m^2)	6.802×10^{-3}
I_{zz} (kg·m^2)	4.548×10^{-6}
l (m)	0.15546
C_d	1
A (m^2)	0.025
ρ_{air} (kg/m^3)	1.22
r_{cop} (m)	$[0\ 0\ 0.05]^T$
r_{susp} (m)	$[0\ 0\ 0.02]^T$
m_p (kg)	0.073

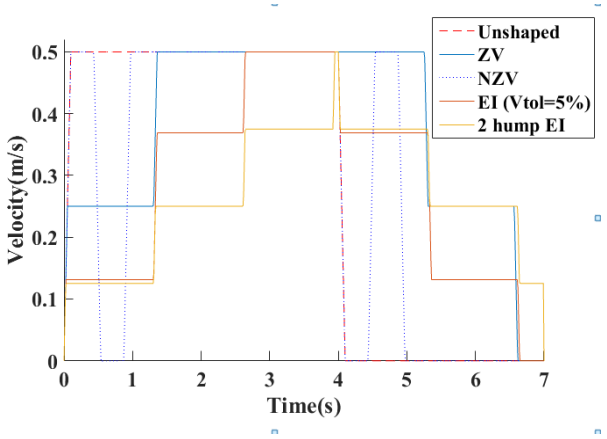

Fig. 9. Velocity profiles

4. SIMULATION RESULTS

While performing the simulations, we set a limitation of 0.5 (m/s) on the maximum translational velocity and 5 (m/s^2) on the maximum translational acceleration of the quadrotor because real quadrotors cannot instantaneously respond to a bang-bang command. In these simulations, the quadrotor followed a straight trajectory which is 2 m long in the y-direction. Five different input shapers were designed to suppress the oscillation of a payload with a cable length of L_p=0.5 (m). The velocity profiles of the quadrotor for the unshaped and shaped commands are shown in Fig. 9.

The effect of L_p on the residual oscillation amplitude in the direction of motion (y-direction) is shown in Fig. 10. Figure 10 shows the payload angles as seen from the body frame. As shown in Fig. 10, all the shapers significantly suppress residual oscillation. The results highlight the improved robustness of the EI and the 2-EI input shapers with respect to the ZV, and the NZV input shapers [Singhose et al. (1997a),Singhose et al. (1997b)]. Fig. 10 shows that as the payload length diverges away from the design payload length both the ZV and NZV shapers show

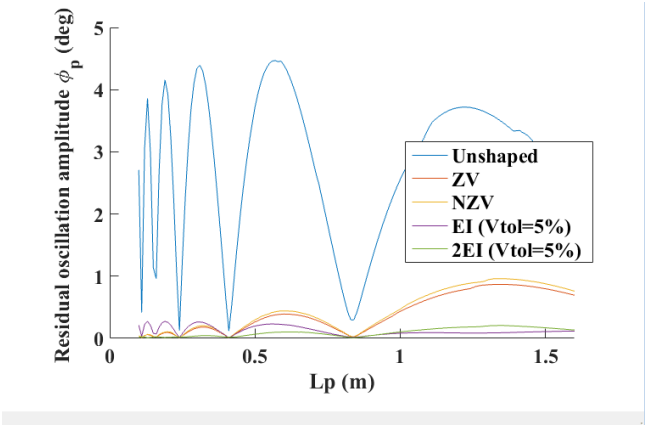

Fig. 10. The effect of L_p on residual oscillation amplitude

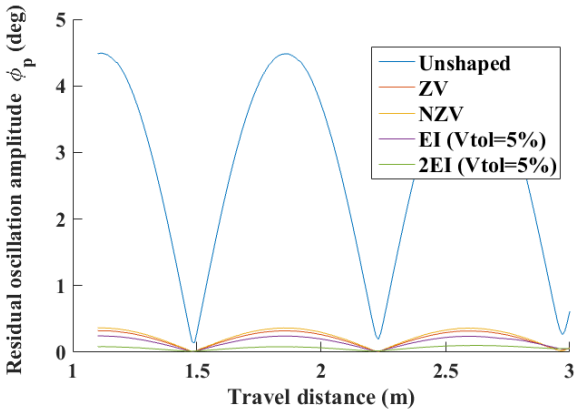

Fig. 11. Effect of travel distance on the residual oscillation amplitude.

greater residual oscillation, while the EI and the 2-EI shapers can still suppress most of it. In addition, the NZV shaper shows less robustness to modeling errors than the ZV shaper as has been shown in earlier literature [Singhose et al. (1997a)].

Although the amplitude of oscillation is minimized at multiples of Td for every case, overall models with input shaping result in lower oscillation than the model without shaping. The effect of travel distance on the residual vibration amplitude is shown in Fig. 11. The residual vibration amplitude varies periodically depending on the travel distance. This periodic nature is caused by the time difference between the two pulses in acceleration that form the trapezoidal velocity profile. The residual vibration amplitude is minimum when this period of time is a multiple of T_d.

5. CONCLUSIONS

The main objective of this study was to implement input shaping within a quadrotor control system and verify that it can reduce oscillation of a cable-suspended payload attached to a quadrotor. A quadrotor with a suspended payload dynamic model was developed and several types of input shapers were applied to velocity control of the quadrotor. The numerical simulations show that implementing input shaping within velocity control succeeded in reducing the payload oscillation.

REFERENCES

Derafa, L., Madani, T., and Benallegue, A. (2006). Dynamic modelling and experimental identification of four rotors helicopter parameters. In *IEEE International Conference on Industrial Technology, Mumbai, India*, 1834–1839.

Homolka, P., Hromčík, M., and Vyhlídal, T. (2017). Input shaping solutions for drones with suspended load: First results. In *21st International Conference on Process Control (PC), Strbske, Slovakia*, 30–35.

Johnson, N.A. (2017). *Control of a Folding Quadrotor with a Slung Load Using Input Shaping*. Ph.D. thesis, Georgia Institute of Technology.

Klausen, K., Fossen, T.I., and Johansen, T.A. (2017). Nonlinear control with swing damping of a multirotor uav with suspended load. *Journal of Intelligent & Robotic Systems*, 1–16.

Sadr, S., Moosavian, S.A.A., and Zarafshan, P. (2014). Dynamics modeling and control of a quadrotor with swing load. *Journal of Robotics*, 2014.

Singer, N.C. and Seering, W.P. (1990). Preshaping command inputs to reduce system vibration. *Journal of dynamic systems, measurement, and control*, 112(1), 76–82.

Singhose, W., Seering, W., and Singer, N.C. (1997a). Time-optimal negative input shapers. *Journal of Dynamic Systems, Measurement, and Control*, 119(2), 198–205.

Singhose, W., Seering, W., and Singer, N. (1994). Residual vibration reduction using vector diagrams to generate shaped inputs. *ASME Journal of Mechanical Design*, 116(2), 654–659.

Singhose, W.E., Porter, L.J., Tuttle, T.D., and Singer, N.C. (1997b). Vibration reduction using multi-hump input shapers. *Journal of dynamic systems, Measurement, and control*, 119(2), 320–326.

Smith, O.J. (1958). Feedback control systems. *NewYork: McGraw-Hill Book Co.*, 331–345.

Tallman, G. and Smith, O. (1958). Analog study of dead-beat posicast control. *IRE Transactions on Automatic Control*, 4(1), 14–21.